A01-28162

AIAA 2001-1923

AN ARCC ENGINE POWERED SPACEPLANE

T. Yamanaka, M. Maita, T. Mori, T. Tsuchiya and O. Okamoto

National Aerospace Lab. Tokyo, Japan

10th International Space Planes and Hypersonic Systems and Technologies Conference

24-27 April 2001

Kyoto, Japan

AIAA 2001-1923

AN ARCC ENGINE POWERED SPACEPLANE

T. Yamanaka*, M. Maita**, T. Mori**, T. Tsuchiya** and O. Okamoto**
National Aerospace Lab. Tokyo, Japan

ABSTRACT

An ARCC (Airbreathing/Rocket Combined Cycle) engine system is assessed for the SSTO (Single-Stage-to-Orbit) capability by flight simulation. For LEO (Low Earth Orbit) missions, a vehicle and propulsion system geometry is designed. The ascent trajectory, the ARCC engine operational conditions along the trajectory, aerodynamics and the trajectory guidance and control of the vehicle are discussed. The ratio of weight in orbit to the jetliner class TOGW (Take-Off Gross Weight) is shown to be excellent for the vehicle to LEO missions.

INTRODUCTION

Reusable STS (Space Transportation System) are conceptually categorized into all-rocket SSTO, TSTO (Two-Stage-to-Orbit), and combined-engine SSTO. All-rocket SSTO carries more than 90% propellant weight fraction to the LOGW (Lift-Off Gross Weight), which requires advanced composite cryogenic tank structures. If 10-20 Mg is assumed for the payload, the vehicle size becomes huge likely as the LOGW over 2,000 Mg. The propellant weight fraction of all-rocket TSTO is about 80%. Even if airbreathing engines such as turbo, RAM and SCRAM jet engines are integrated to the fly-back booster, the propellant weight fraction are lower than the all-rocket SSTO by about 10%, however, the development cost is estimated to be much higher than the SSTO. Several cost analyses report that the operational cost of TSTO will be 1/4～1/3 to the expendable rockets including refund for investment[1,2].

Viable and practical airbreathing, hypersonic propulsion systems for fully reusable SSTO have been primarily interested in for these more than fifteen years. Two typical concepts were recently studied, i.e., CTSC (Combined Turbine Scramjet Cycles) powered HTHL-SSTO[3] and RBCC (Rocket Based Combined Cycle) powered VTHL-SSTO[4]. The propellant weight fraction to the 1.0Mlb TOGW of slush H2 CTSC-SSTO is about 75%, and that to the 1.648Mlb LOGW of slush H_2 RBCC-SSTO is 79.86%. If these concepts are assumed for future fully reusable human-rated SSTO to the ISS (international Space Station) mission, however, much higher reliability and much lower operational cost will be little hopeful for them comparing to the current Space Shuttle.

The authors presented a propulsion engine concept called ARCC (Airbreathing/Rocket Combined Cycle) engine for space planes in the last 9th International Space Planes and Hypersonic Systems and Technologies Conference in Norfolk, VA., Nov., 1999[5]. Two kinds of computer programs were developed to calculate an ARCC engine performance. One is for lower flight velocities from takeoff/liftoff to about M_∞～3, which was modified later by taking into account the boundary layer effects to the engine internal parts together with active cooling to the air combustion chamber[6]. Another was for higher flight

*Technical Advisor, AIAA Associate Member

**Spaceplane Research Group

velocities with transpiration cooling by fuel hydrogen to all parts of engine internal surfaces (except ramp and body expansion nozzle). Numerical results showed excellent performance until very high flight vehicle velocities.

This paper presents a numerical result of flight performance of an ARCC engine powered SSTO vehicle. The primary purpose is to estimate launching capability of the vehicle. A reference numerical vehicle is designed for calculating easily the vehicle mass properties, aerodynamics, and the performance of the ARCC engine. A computer code is newly developed to calculate subsonic, transonic, supersonic, and hypersonic aerodynamics including body nozzle expansion flow for the propulsive lifting body type vehicle. A flight simulation computer program is also developed, which integrates the related programs such as vehicle geometry, propulsion system geometry, aerodynamics and the ARCC engine codes.

ARCC ENGINE

Propulsion System Concept

An airbreathing engine for SSTO vehicles must be evaluated its performance along the flight trajectories together with the vehicle configuration, because the engine characteristics are closely related with the vehicle configuration. Figure 1 shows a schematic of the reference vehicle.

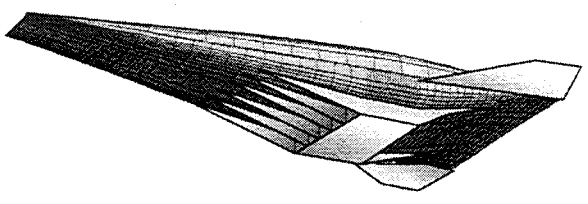

Fig. 1 Schematic of the Reference Vehicle

The prime author believes that the propulsion system concept should be simple. Therefore, variable geometry should be least to use for the air intake, engine internal flows such as the diffuser, air combustor, and body nozzle. Figure 2 shows two side schematics of the propulsion concept. A rocket engine is contained in each strut as the Strutjet[4]. A rocket engine, however, it plays various roles in the ARCC engine. The first is as rocket engine it self. The second is as ejector to draw air in the forward part of mixing between rocket exhaust gas and the incoming air flow from the low subsonic flight velocities to the hypersonic flight velocities exceeding the rocket exhaust velocity of about $V \sim 4000$m/sec, which produces thrust augmentation. The third is as flame holders for fuel/air combustion in the air combustor. The fourth is as hydrogen fuel and oxygen injectors to the air combustor by using lower and higher o/f (mass flow rate of oxygen to mass flow rate of fuel through rocket) compared with those of the conventional LOX/LH_2 rocket engines. The fifth is as pressure controller for air combustor, such as the rocket exhaust gas plays a spontaneous role of adjustable supersonic mixing for supersonic combustion to keep the combustion pressure within reasonable values without variable geometry. The fifth function is unique and important for the ARCC engine specifically to operate in the very high hypersonic atmospheric flight of the SSTO vehicle.

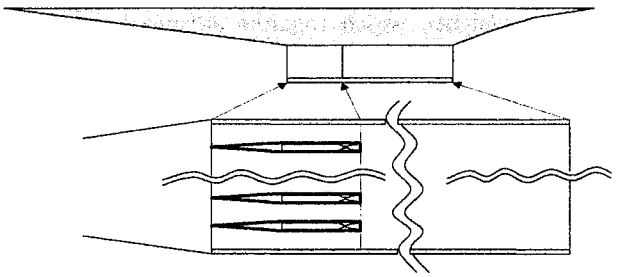

Fig. 2 Schematic of ARCC Propulsion Concept

If one wants to maximize the performance of an airbreathing engine in very high flight Mach numbers, area contraction ratios of the forward air flow passage in front of combustor must be smaller as far as possible, otherwise various internal flow choking phenomena will be induced. The smaller contraction ratio needs the lower pressure combustor, which requires longer combustor to enable for mixing and combustion. If higher contraction ratios (supersonic diffusers) are designed for those parts, the airbreathing engine does not work in very high flight velocities. The exhaust gases of rockets can increase pressure of combustor via mixing processes, which extends simultaneously the maximum flight Mach number of the ARCC scramjet mode with avoiding hypersonic air dissociation effects. This is the fifth unique and important function of rockets in the ARCC engine as the above mentioned.

Thermal management problems are very severe for the Strutjet type RBCC propulsion system, as Siebenhaar stated[7]. In order to avoid the problems, the airbreathing cycle of their Strutjet is limited to lower flight Mach number of about 8. Even if the airbreathing cycle of the Strutjet is limited to the lower flight Mach numbers, the strut and airbreathing combustion chamber wall structures need to be cooled by fuel hydrogen through wall jackets like those of conventional LOX/LH_2 rocket engines, because of high recovery temperatures on the walls. Supposing high thermal conductivity and high stiffness such as copper based composites for the wall structures, the prime author considers transpiration cooling by means of fuel hydrogen to the walls of ARCC engine.

Performance of the ARCC Engine

The ARCC propulsion engine codes are divided into two parts for lower and higher velocities because of the difference of active cooling to the walls of ARCC engine depending on thermal management for flight velocities. One is for flight velocities from takeoff/liftoff to about $M_\infty \sim 3$, in which the engine structures (except fuel/air combustor) are in the limits of high temperature resistance without active cooling. Transpiration cooling is applied only to air/fuel combustion parts in the lower velocity code and to all parts of the engine internal surfaces (except ramp and body nozzle) in the higher velocity code.

Numerical results of the ARCC propulsion engine codes are shown in Figs. 3 and 4. Figures 3-a and 3-b show specific impulses of momentum change thrust versus flight velocity of the lower and higher codes, respectively. The thrust is composed of momentum change and axial pressure balance of the propulsive lifting body type vehicle, the latter is calculated by the aerodynamics codes in the flight simulation program stated in the later section. The o/f (3 for the lower and 10 for the higher flight velocity) and the rocket engine combustion pressure are selected for optimum flight in the flight simulation. Figures 4-a and 4-b show mass flow rates of rocket engine (mfrr), hydrogen wall cooling (mfrhwc), and internal air (mfra) of the lower and higher flight velocity codes, respectively. It must be noted that the hydrogen fuel to air mass ratios in the fuel/air combustion are lean in the lower flight velocities and very rich in the higher flight velocities, compared with the stoichiometric mixture. If we consider overall propulsive efficiencies, fuel lean combustion in the lower flight velocities is desirable. While fuel rich combustion in the higher flight velocities is advantageous not only for the overall propulsive efficiency but for the higher exit velocity to the ambient pressure because of lower mean molecular weight of the exhaust gas.

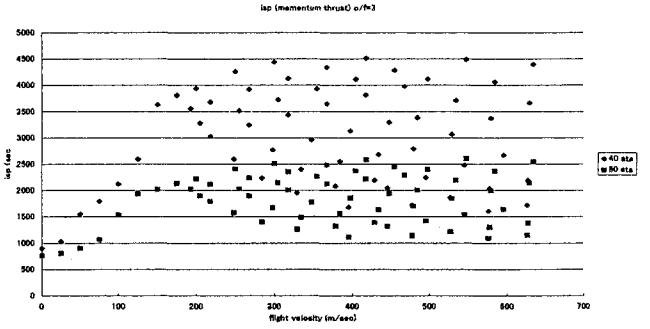

3-a Lower Flight Velocity (o/f=3)

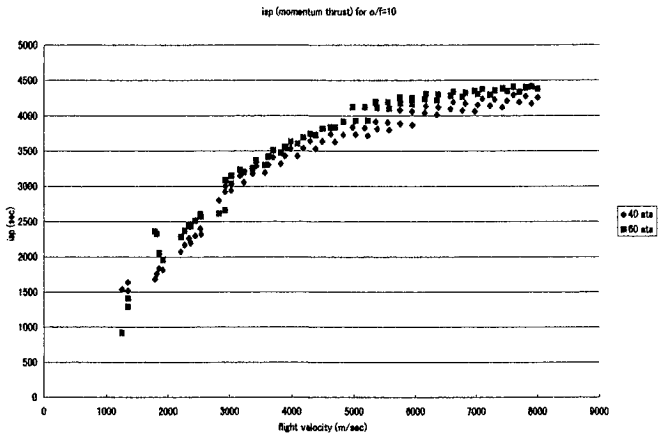

3-b Higher Flight Velocity(o/f=10)

Fig. 3 Specific Impulses vs. Flight Velocity

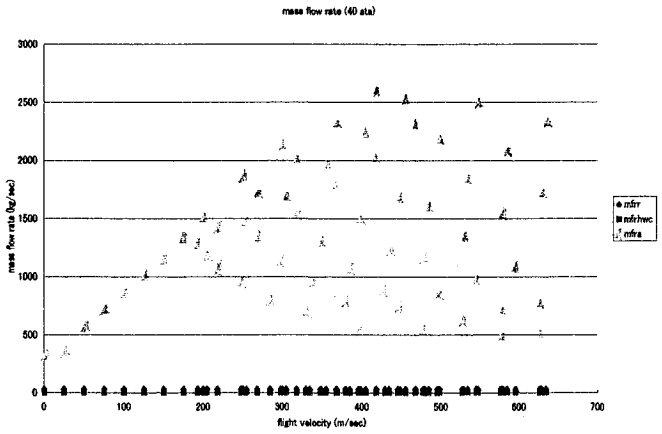

4-a Lower Flight Velocity (40ata & of=3)

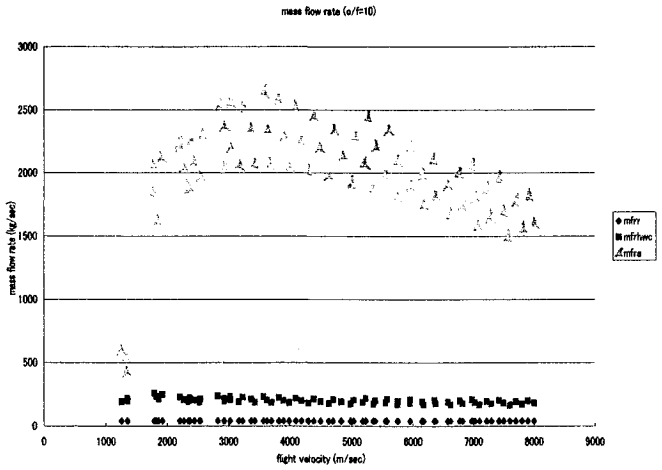

4-b Higher Flight Velocity (40ata & o/f=10)

Fig. 4 Mass Flow Rates vs. Flight Velocity

NUMERICAL VEHICLE

In order to calculate the flight performance of ARCC engine powered vehicles, a numerical vehicle is designed. Every size of the vehicle configuration including ARCC engine geometry is expressed by dimensionless parameters by vehicle body length. Numerical vehicles are easy to re-configure for obtaining optimum flight characteristics in the flight simulation. The body surface is basically composed of two ruled surfaces, upper and under, of which cross sections are elliptic for simplicity with a common major axis, however, the minor axes are different. The minor axis of the upper surface is given by NACA 2412 airfoil along the body axis. The minor axis of the under surface is given by multiplying a scale factor for obtaining a reasonable Kuichmann Tau. Table 1 and Fig. 5 show major specifications of the numerical vehicle used in the flight simulation, respectively.

Table 1 Major Specifications of Numerical Vehicle

Length	72,000	m/m
Nose-width	8,000	m/m
Body Sweep	89	degrees
Body Slender Ratio	0.7609	
Ramp Angle	9	degrees
Engine Height	1,800	m/m
Wing Lead Location	0.618	
Vertical-Tail Lead Location	0.813	
Vertical-Tail Trail Location	0.967	
Planform Area	1,123.76	m^2
Numbers of Struts	3	
Pitch of Strut	2,718.72	m/m
Air Intake Area	14.844	m^2
Engine Weight	8,524.3	kg
Landing Gear Weight	4,864.6	kg
TOGW	380,906	kg
Kuichmann Tau	0.1169	
Propellant Weight Fraction	63.8	%
Initial LOX weight	128,789	kg
Initial LH_2 Weight	114,186	kg

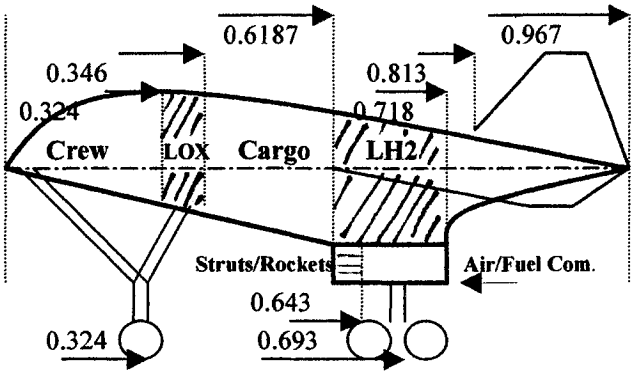

Fig. 5 Numerical Vehicle

For the mass properties of the vehicle such as mass of each component, moment of inertia, and center of gravity, 5m/m thickness aluminum is assumed for all surfaces of body including ramp, nozzle, crew and cargo compartments, cryogenic tanks, wings and vertical tail. 2m/m thickness aluminum is assumed for each partition wall of the crew/Lox-tank, the Lox-tank/cargo-bay, and the cargo-bay/LH2-tank. Combination of 2.5m/m thickness aluminum and 2m/m copper are assumed to the upper base, the sides and the under base of the engine. For the struts containing rocket engines, 2.5m/m thickness aluminum and 2m/m copper are assumed and masses of rocket engine injectors and throats are added to the reasonable locations. Masses of avionics, cryogenic pumps and pipes and the related instrumentation are included in the weights of crew, cargo compartments and contingency. The weight of landing gear is estimated by $129.0[W_{to}(lb)x10^{-3}]^{-0.66}$ according to the USN weight estimation method[8].

AERODYNAMICS and NOZZLE FLOW

The calculation of aerodynamics for propulsive lifting body and body nozzle flow were most difficult problems for our work, because there were no available data base and computation codes. The prime author developed them. The aerodynamic codes are split into four parts, i.e., subsonic, transonic, supersonic, and hypersonic. The method is basically CFD. The three-dimensional perturbation velocity potential linearized differential equation is numerically solved over the surfaces of the lifting body for compressible subsonic, transonic and supersonic flow. The aerodynamic database of wings and vertical tail are provided by the available references[9,10,11,12,13]. Hypersonic aerodynamic data are calculated based on the Newtonian flow model for lifting body, wings and vertical tail.

The previously stated ARCC engine codes calculate only thrust of momentum change (Figs. 3-a and 3-b). The contribution of nozzle wall pressures to the thrust must be calculated in the body nozzle expansion flow, which contributes simultaneously to the lift force. Assuming the Prandtle-Meyer expansion of the engine exit flow at the cowl exit to the ambient air and approximating half-free jet boundary adjusting the pressure to the ambient air pressure[14], body nozzle expansion flow is calculated in both cases of full flow and incomplete expansion flow. The code of body nozzle expansion flow is quasi-three-dimensional because the basically two-dimensional expansion flow model is extended to the transverse sides by considering a fairly large aspect ratio of engine exit of 4.73. The whole surface of the lifting body is divide by 254x360 small panels, on which aerodynamic and gas-dynamic equations are solved to estimate pressures.

FLIGHT SIMULATION

A flight simulation program is developed for estimating mission capability of the ARCC engine powered SSTO vehicle, which process is described in Fig. 6. Vehicle geometry is firstly given. Then, optimization of strut array and estimation of TOGW including landing gear are performed. After giving rocket engine detailed specifications such as throat, rocket nozzle expansion ratio, efficiencies of rocket and fuel/air combustion, and body nozzle exit efficiency, the flight simulation starts. Flight codes are split into seven phases, i.e., ground-run, head-up-ground-run, subsonic ascent of very low flight

dynamic pressures, transonic flight, through sonic barrier flight, supersonic sonic flight, and hypersonic flight. The first six codes are described in the orthogonal coordinates, however, the last is expressed in the geocentric polar coordinates toward orbital missions. In each phase, peculiar guidance and controls are carried out for the rocket engine o/f, the rocket engine combustion pressure, attack angle of the vehicle attitude to meet the required constraints to the vehicle such as trajectory dynamic pressure and axial acceleration.

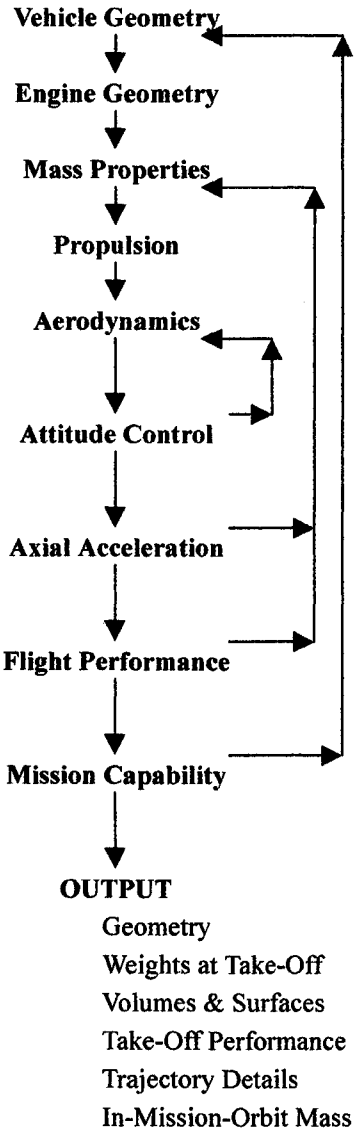

Fig. 6 Flight Simulation Program

Table1 shows a typical synthesized configuration based on the repeated flight simulations with sizing. Table 2 shows the output of the flight simulation. In the Table 2, the final injection means the terminal state of the ARCC engine operation, and the true anomaly is measured from the launching site. After the terminal state, two missions of 1,000km and 10,000km altitude circular orbits are calculated, where the Hohmann transfer orbits are used by means of OME (Orbital Maneuvering Engine) burning. The 1,000-km-orbit mission corresponds actually to the 500-km-orbit ISS mission because of going and returning to the atmospheric reentry. The specific impulse of the OME is assumed as 450 seconds of LOX/LH_2. Detailed analyses of returning and atmospheric reentry trajectory are beyond the present paper.

Figure 7 shows the trajectory in terms of altitude versus flight velocity. An OME burning maneuver is required to accelerate the vehicle, from the flight velocity of 475m/sec at altitude of 17.5km to the flight velocity of 1,514m/sec at altitude of 25.6km. This is because of transition problem from the lower velocity ARCC engine code to the start of the higher velocity ARCC engine code. Figures 8 shows the rocket engine combustion pressure along the trajectory, where mixture ratios of rocket engine are selected for optimization of the ARCC engine operation as o/f=3 for the lower velocity engine code and o/f=9 for the higher velocity engine code, respectively. Figure 9 shows specific impulses of the momentum thrust (isp) and of the effective thrust (eisp) calculated by aerodynamics and the body nozzle expansion flow analysis, respectively. The o/f of rocket engine are based on the higher isp operation of the pre-estimated data referred by Fig.3. The rocket engine combustion pressure depends deeply on the vehicle axial acceleration together with attack angle. The effective isps are, however, very low during transonic to supersonic flight velocity regions. Figure 10 shows vehicle mass to TOGW versus flight velocity. The figure shows excellent mission capability of the

Table 2 Output of Flight Simulation

Take-Off	
Take-Off Ground Distance	2,486 m
Take-Off Speed	220 m/sec
Take-Off Distance (z>=body length)	4,450 m
Terminal of the ARCC Engine	
Altitude at Final Injection	44.5 km
True Anomaly at Final Injection	2.99 degrees
Vehicle Mass at Final Injection	245,995 kg
Crew Payload	1,941 kg
Cargo Payload	45,433 kg
Propellant Mass	99,734 kg
1,000km Altitude Circular Orbit Mission	
Vehicle Mass in 1,000km Orbit	207,530 kg
Cargo Payload	45,433 kg
+ (Contingency)	38,432 kg
Remaining Propellants	22,837 kg
LOX	17,128 kg
LH2	5,709 kg
10,000km Altitude Circular Orbit Mission	
Vehicle Mass in 10,000km Orbit	124,356 kg
Cargo Payload	14,395 kg
Remaining Propellants	9,134 kg
LOX	6,851 kg
LH2	2,283 kg

ARCC engine powered SSTO until very high flight velocity.

Figures 11-13 show, flight dynamic pressure, aerodynamic and propulsive forces, and vehicle axial acceleration, respectively. The axial acceleration is controlled by rocket engine combustion pressure and by angle of attack under 6g. If one wants to decrease the axial acceleration to much lower levels, configuration analyses will be required, which is stated in the next section. The lift becomes very high in the hypersonic flight velocity region, especially beyond 4,500m/sec. Such very high lift will induce difficult guidance and control problems for the vehicle, which are beyond the present paper. Even if the OME is ignited at the velocity region of 4,500m/sec, however, the mission capability of the ARCC engine powered SSTO vehicle to the ISS orbit is well described.

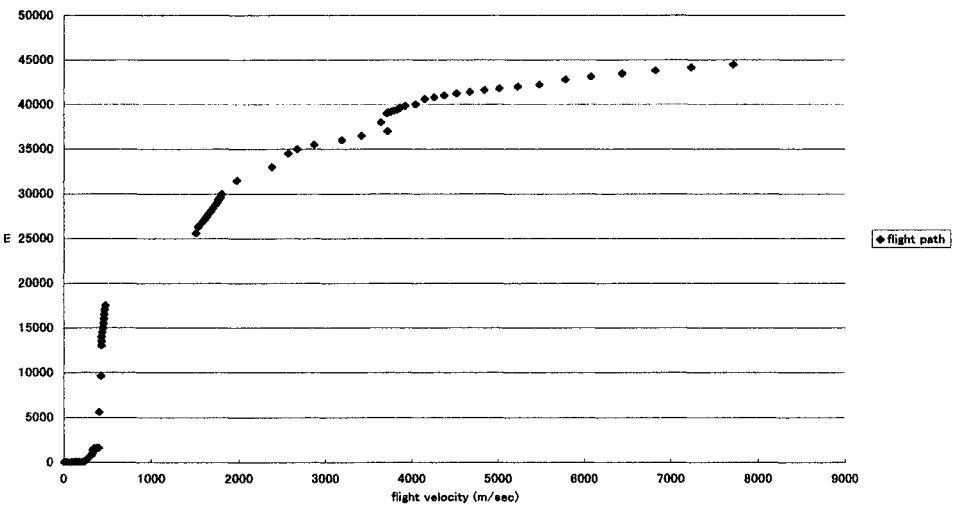

Fig. 7 Trajectory Altitude vs. Flight Velocity

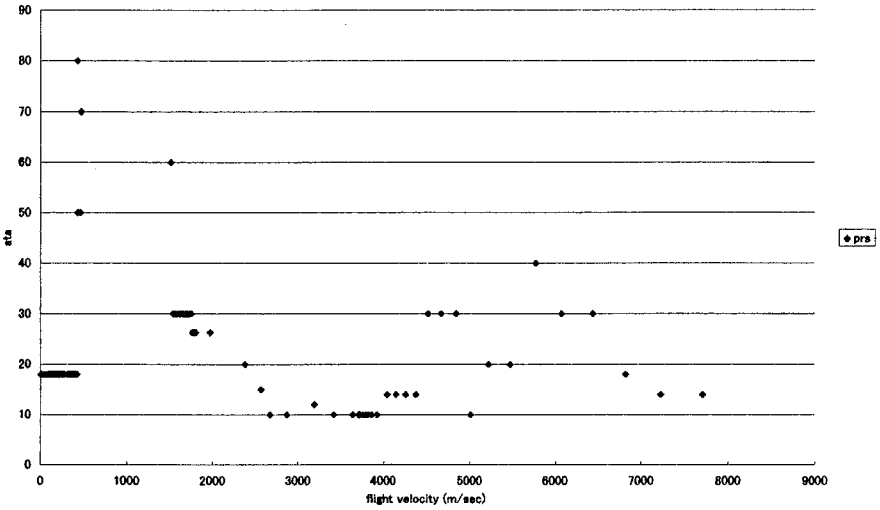

Fig. 8 Rocket Combustion Pressure

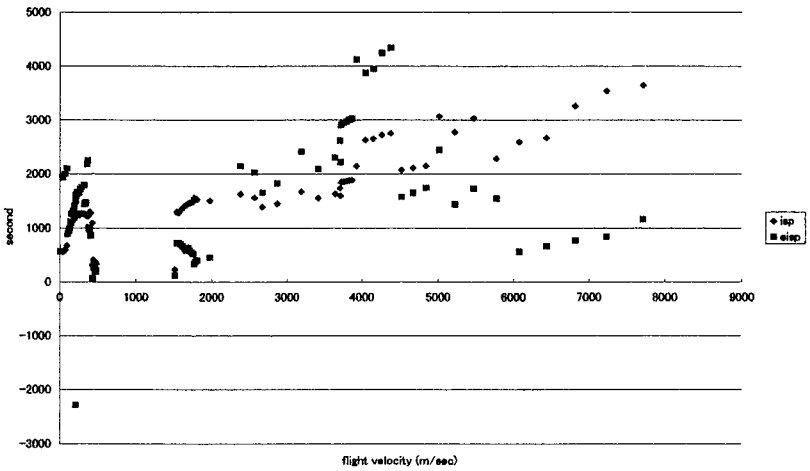

Fig. 9 Specific Impulses of Momentum Thrust and Effective Thrust

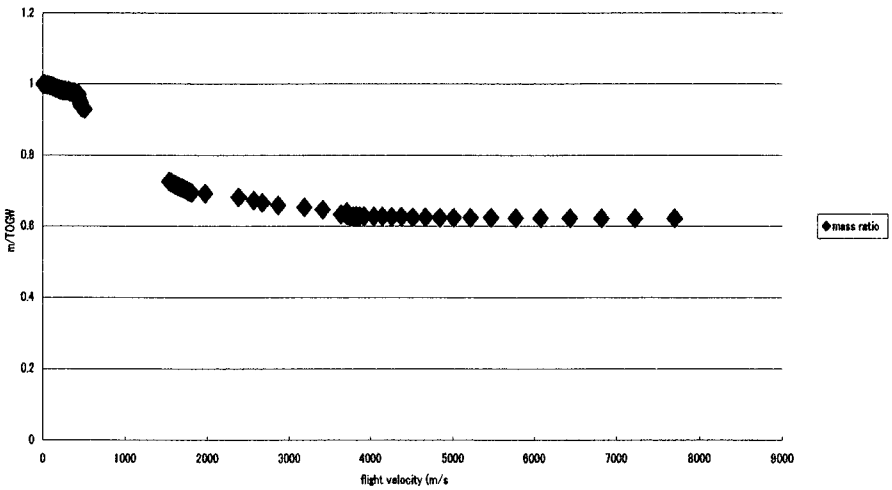

Fig. 10 Mass Ratio to TOGW

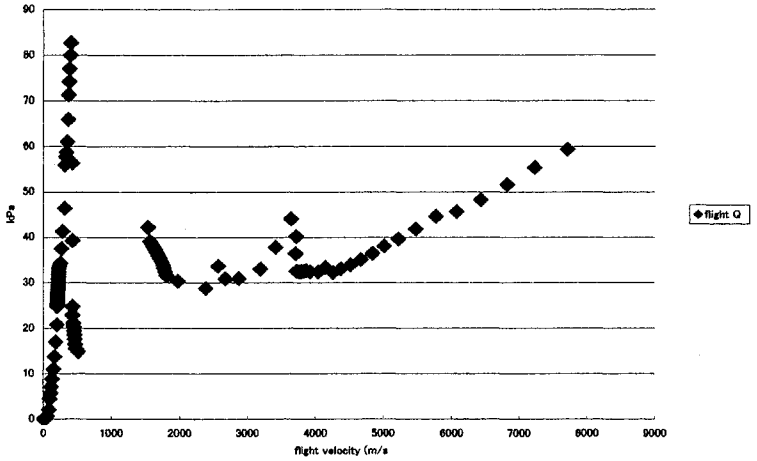

Fig. 11 Trajectory Dynamic Pressure

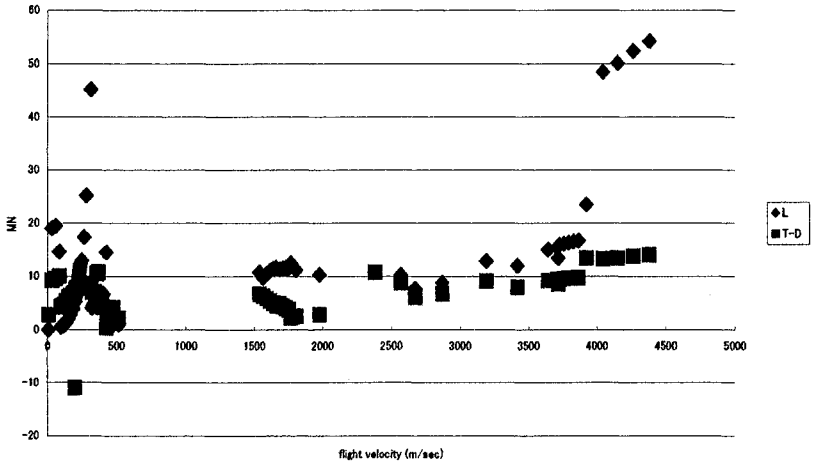

Fig. 12 Aerodynamics and Propulsion Forces

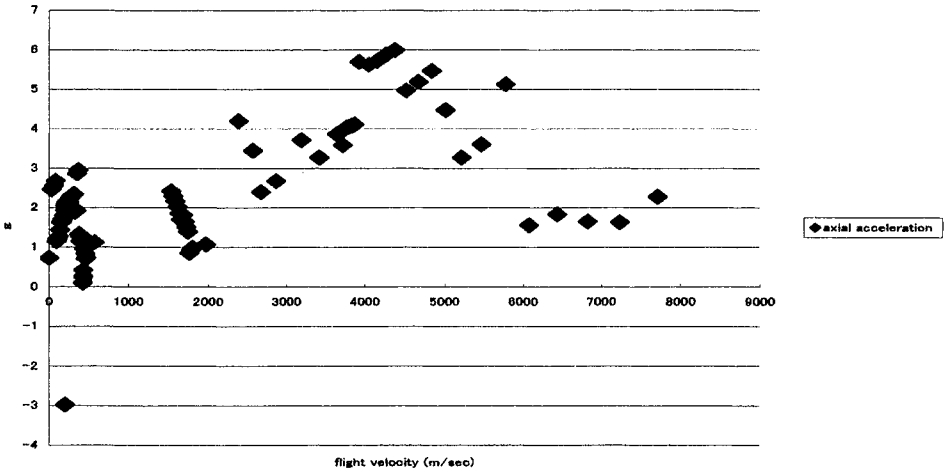

Fig. 13 Vehicle Axial Acceleration

CONCLUDING REMARKS

The primary objective of this paper is to find out vehicle design problems specifically relating to matching with propulsion system by assessing launching capability of an ARCC engine powered SSTO configuration. The flight simulation was like a continuous numerical wind tunnel test from take-off to the limit of flight velocity for the ARCC engine operation. Transonic and hypersonic flights are required very sophisticated guidance and control of the vehicle, however, the maneuvers were simplified by adjusting the altitude versus the obtained flight velocity with given attack angles in the flight simulation. The followings are findings of the flight simulation.

(1) The mission capability of the vehicle is found to be excellent, which are going to the ISS orbit from take-off and returning to ground and higher altitude orbits with reasonable payload.

(2) The ARCC engine codes have a transition problem such that the OME burning is required for acceleration from the lower to the higher flight velocity. The prime author supposes that this comes from partly owing to the ARCC engine matching with vehicle configuration and mainly because of rocket engine nozzle expansion. This will be studied in future.

(3) Acceleration phases through sonic barrier, supersonic RAM, and hypersonic SCRAM flight with very high lift induce a contradictory rocket engine operational problem. The acceleration phase through sonic barrier needs larger thrust by means of high rocket engine combustion pressure, while the supersonic RAM flight phase requires lower rocket engine combustion pressure for the purpose of decreasing the body nozzle expansion flow pressure under a constraint of the axial acceleration limit. The hypersonic flight phase needs larger thrust, which must be performed, however, by the lower rocket engine combustion pressure because of SCRAM operation. If the higher rocket engine combustion pressure is used for this phase, the ARCC engine SCRAM mode does hardly work, because the rocket engine exit plumes inhibit supersonic mixing with incoming supersonic flow of air. To solve this problem through these flight phases, variable throat width is applied in this flight simulation, which violates the author's principle toward the SSTO propulsion system design of non-variable geometry for simplicity stated in the references [5] and [6]. The authors believe that this problem might be solved by partial operation of multi strut-rocket engines, which is also necessary for one-engine-out operation during take-off flight. The partial operation of multi strut-rocket engines will be studied in future.

(4) The lower rocket engine combustion pressure operation during hypersonic SCRAM mode flight induces still larger axial acceleration, which is solved by a larger attack angle of vehicle attitude control. A larger attack angle of vehicle attitude control induces, however, very high lift. A much sophisticated guidance and control of the vehicle flight will be needed.

(5) The NACA 4412 airfoil is tentatively selected for the vehicle configuration, however, this configuration induces several flight control problems in the transonic, supersonic and hypersonic flight regions as previously stated. Another airfoil to the lifting body such as much more for supersonic and for hypersonic, must be studied for the ARCC engine powered SSTO vehicle.

REFERENCES

1. Ksotromin, S. F., "COST EFFECTIVENESS ESTIMATES OF THE PARTIALLY REUSABLE LAUNCHERS FAMILY WITH UNIFORM COMPONENTS", AIAA-99-4887, 1999
2. Olds, J.R., et al., "Sargazer:A TSTO Bantax-X VEHICLE CONCEPT UTILIZING ROCKET-BASED COMBINED-CYCLE PROPULSION", AIAA 99-4888, 1999
3. Moses, P. L., et al., "An Airbreathing Launch Vehicle Design with Turbin-Based Low-Speed Propulsion and Dual Mode Scramjet High-Speed Propulsion", AIAA 99-4948, 1999
4. Stemler, J. N., et al., "ASSESSMENT of RBCC-POWERED VTHL SSTO VEHICLES", AIAA 99-4947, 1999
5. Yamanaka, T., et al., "AIRBREATHER/ROCKET COMBINED CYCLE (ARCC) ENGINE FOR SPACEPLANES", AIAA 99-4812, 1999
6. Yamanaka, T., "Innovative Breakthroughs to a Reusable STS", The Space Transportation Market: Evolution or Revolution?, Proceedings of an International Symposium, 24-26 May 2000, Strasbourg, France, Kluwer Academic Publishers, Dordrecht, The Netherlands, January 2001, pp. 167-175
7. Siebenhaar, A. and Bulman, M. J., "The Strutjet Engine: The Overlooked Option For Space Launch", AIAA 95-3124, 1995
8. Nicolai, L. M., "Fundamentals of AIRCRAFT DESIGN", METS, Inc., California, 1985, p. 20-5
9. ditto, CHAPTER 2, 9, 11, APPENDIX E, and G
10. Jones, R. T., "PROPETRIES OF LOW-ASPECTRATIO POINTED WING AT SPEEDS BELOW AND ABOVE THE SPEED OF SOUND", NACA TR-835, 1946
11. Malvestuto, F. S. et al., "THEORETICAL LIFT AND DAMPING IN ROLL AT SUPERSONIC SPEEDS OF THIN SWEPTBACK TAPERED WINGS WITH STREAMWISE TIPS, SUBSONIC LEADING EDGES, AND SUPERSONIC TRAILING EDGES", NACA TR-970, 1960
12. Cohen, D., "FORMULAS FOR THE SUPERSONIC LOADING, LIFT, AND DRAG OF FLAT SWEPTBACK WINGS WITH LEADING EDGES BEHIND THE MACH LINES", NACA TR-1050, 1951
13. McDevitt, J. B., "A CORRELATION BY MEANS OF TRANSONIC SIMILARITY RULES OF EXPERIMENTALLY DETERMINED CHARACTERISTICS OF A SERIES OF SYMMETRICAL AND CAMBERED WINGS OF RECTANGULAR PLAN FORM", NACA TR-1253, 1956
14. Adamson, Jr., T. C., et al., "On the Structure of Jets From Highly Underexpanded Nozzles Into Still Air", J. Aero/Space S., January, 1959, pp. 16-24